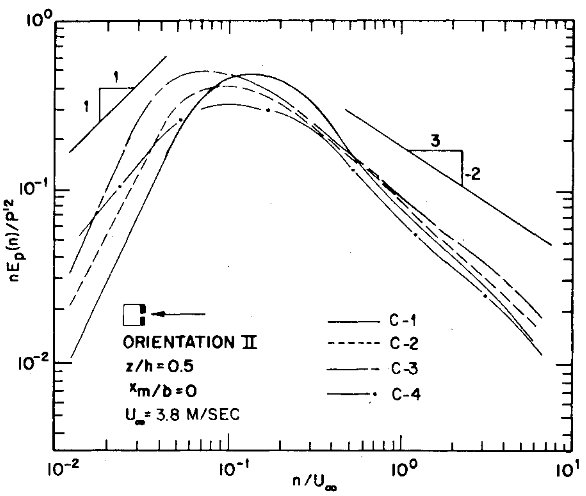

Fig. 3 Normalized spectra of pressure fluctuations on upstream face of building at half the building height.

Such waves could possibly be excited by the fan or the various turbulence manipulators. Batchelor reported[2] on similar waves in one of his experiments with wind tunnels. Therefore, for the signals to be in phase for all sound frequencies present in the tunnel the sound probe must be near the model of the building being tested in the simulated layer.

Based on these findings, the sound probe was mounted in the sidewall of the test section, close to the tunnel floor, (see Fig. 3 of Ref. 4). Because of the size of the sensing region of the probe, and its location upstream of the model, no detectable influence of the static pressure fluctuations in the boundary layer on the sound signal was found to occur within the frequencies of interest.[3]

The final tuning of the subtraction system was done while the tunnel was operating under the model testing conditions. This involved the fine matching of the signal amplitudes, by adjusting the gain of the amplifier in the sound probe leg of the subtraction circuit, Fig. 1, in order to make the rms of the subtracted output a minimum. This optimum setting was found to be the same for all test conditions.

In some cases, the tuned subtraction system provided a total reduction in the rms of the model pressures of as much as 80%. The left portion of Fig. 2 displays the autocorrelated outputs of the low-frequency portion of the nonsubtracted and the sound-subtracted output from the building model. Before the sound subtraction, well-defined frequencies corresponding to the sound contamination in the signal are noted. With the aid of the sound-subtraction scheme, however, Fig. 2 reveals the removal of the sound pressure contaminant. Oscilloscope traces of the nonsubtracted and subtracted model outputs while operating under a testing condition are shown in the bottom part of Fig. 2. In order to compare these signals one should note that because of the oscilloscope scale setting, the amplitude of the nonsubtracted output of the building model is actually twice as large as displayed. Figure 2 indicates how well the subtraction system performs in removing the sound pressure contamination from the signal. This technique therefore provides us with a signal from which we can make accurate and reliable fluctuating pressure measurements on building models. An example of the type of unsteady pressure measurements made possible by this technique is shown in Fig. 3.

Acknowledgment

This work was supported under NSF Grant ENG 76-04112.

References

[1] Hunt, J.C.R. and Fernholz, H., "Wind-Tunnel Simulation of the Atmospheric Boundary Layer: A Report on Euromeck 50," *Journal of Fluid Mechanics,* Vol. 70, Pt. 3, Aug. 1975, pp. 543-599.

[2] Batchelor, G.K., "Sound in Wind Tunnels," Australian Council for Aeronautics Rep. ACA-18, 1945.

[3] Corke, T.C. and Nagib, H.M., "Sensitivity of Flow Around and Pressures On a Building Model to Changes in Simulated Atmospheric Surface Layer Characteristics," Illinois Inst. of Technology, Chicago, Ill., Fluids and Heat Transfer Rept. R76-1, 1976 (available from NTIS as publication Pb267909/AS).

[4] Corke, T.C. and Nagib, H.M., "Unsteady Pressure Measurements in a Low-Speed Wind Tunnel Using a Large Signal-To-Noise Technique." Proceedings of AIAA 10th Aerodynamic Testing Conference, San Diego, Calif., April 1978, p. 492.

Bessel Function Evaluation of the Clamped End Bending Moment of an Impulsively Loaded Beam

Henry E. Fettis*
Mountain View, Calif.

IN a recent Note by Sagartz and Forrestal,[1] dealing with stresses in an impulsively loaded, semi-infinite beam, the following expression was obtained for the bending moment at the clamped end:

$$\frac{M}{Lrc_b} = \frac{2\alpha}{\pi}\int_0^\alpha \frac{(\alpha^2-\rho^2)^{1/2}\sin\rho_\tau}{[\alpha^2-(1-\gamma)\rho^2]\rho}\,d\rho \tag{1}$$

(for the significance of the various parameters, see Ref. 1.) In the present Note, we show that Eq. (1) can be given in terms of Bessel functions and Bessel function integrals.

The change of variable, $\rho=\alpha\cos\theta$, reduces Eq. (1) to the following

$$\frac{M}{Lrc_b} = \frac{2}{\pi}\int_0^{\pi/2} \frac{\sin(z\cos\theta)\sin^2\theta}{\cos\theta[1-(1-\gamma)\cos^2\theta]}\,d\theta$$

$$=y_1(z)-\gamma y_2(z) \tag{2}$$

where $z=\alpha\tau$, and

$$y_1(z)=\frac{2}{\pi}\int_0^{\pi/2}\frac{\sin(z\cos\theta)}{\cos\theta}\,d\theta \tag{3a}$$

$$y_2(z)=\frac{2}{\pi}\int_0^{\pi/2}\frac{\sin(z\cos\theta)\cos\theta}{1-(1-\gamma)\cos^2\theta}\,d\theta \tag{3b}$$

By differentiation

$$\frac{dy_1}{dz}=J_0(z) \tag{4}$$

$$(1-\gamma)\frac{d^2y_2}{dz^2}+y_2=J_1(z) \tag{5}$$

where use has been made of the following integral representations for the Bessel functions $J_0(z)$ and $J_1(z)$ (Ref. 2):

$$J_0(z)=\frac{2}{\pi}\int_0^{\pi/2}\cos(z\cos\theta)\,d\theta$$

Received Feb. 13, 1978. This paper is declared a work of the U.S. Government and therefore is in the public domain.
Index category: Structural Dynamics.

*Consultant.

$$J_1(z) = \frac{2}{\pi}\int_0^{\pi/2} \sin(z\cos\theta)\cos\theta d\theta$$

Thus, with the initial values

$$y_1(0) = 0 \tag{6a}$$

$$y_2(0) = 0, \quad y_2'(0) = \frac{1}{\sqrt{\gamma}(1+\sqrt{\gamma})} \tag{6b}$$

we find that

$$y_1(z) = \int_0^z J_0(t)\,dt \tag{7}$$

$$y_2(z) = \frac{\sqrt{(1-\gamma)}}{\sqrt{\gamma}(1+\sqrt{\gamma})}\sin\frac{z}{\sqrt{(1-\gamma)}} + \frac{1}{\sqrt{(1-\gamma)}}\int_0^z \sin\frac{z-t}{\sqrt{(1-\gamma)}} J_1(t)\,dt \tag{8}$$

Finally, after integrating the last term in Eq. (8) by parts,

$$\frac{M}{Lrc_b} = \int_0^z J_0(t)\,dt - \sqrt{\frac{\gamma}{(1-\gamma)}}\sin\frac{z}{\sqrt{1-\gamma}} + \frac{\gamma}{1-\gamma}\int_0^z \cos\frac{z-t}{\sqrt{1-\gamma}} J_0(t)\,dt \tag{9}$$

Integrals of the type in Eq. (7), which can be expressed in terms of Bessel and Struve functions,[2] are available in trabulated form.[3] Those in Eq. (9) are known as Schwartz integrals, and are discussed in some detail elsewhere.[4-6]

For values of γ in the vicinity of unity, a computationally more tractible form can be obtained by expanding the denominator of Eq. (3), and using the following formula (obtained from Poissons integral representation[2] by differentiation):

$$\int_0^{\pi/2} \sin(z\cos\theta)\sin^{2n}\theta\cos\theta d\theta = \frac{\pi}{2}\,\frac{1\cdot 3\ldots(2n-1)}{z^n}\,J_{n+1}(z)$$

The resulting expression is

$$\frac{M}{Lrc_b} = \int_0^z J_0(t)\,dt - J_1(z) + \frac{(1-\gamma)}{\gamma}\,\frac{J_2(z)}{z} - 1\cdot 3\left[\frac{1-\gamma}{\gamma}\right]^2\frac{J_3(z)}{z^2} + \ldots +$$

Acknowledgment

This work was supported in part by the Air Force Flight Dynamics Lab., Wright-Patterson Air Force Base, Ohio.

References

[1]Sagartz, M. J. and Forrestal, M. J., "Bending Stresses Propagating from the Clamped Support of an Impulsively Loaded Beam," *AIAA Journal*, Vol. 10, Oct. 1972, pp. 1373-1374.

[2]Magnus, W. and Oberhettinger, F., *Formeln und Satze fur die speziellen Funktionen der mathematischen Physik*, Springer, New York, 1948, Sec. III.

[3]Abramowitz, M. and Stegun, I., *Handbook of Mathematical Functions*, Dover, New York, 1965, Table 11.1.

[4]Schwartz, L., "Untersuchung Einiger mit der Zylinderfunktionen nullter Ordung verwandter Funktionen," *Luftfahrtforshung*, Bd. 20, Lfg. 12, Feb. 1944, pp. 341-372.

[5]Bisplinghoff, R. L., Ashley, H., and Halfman, R. L., *Aeroelasticity*, Addison-Wesley, Reading, Mass., 1955.

[6]Agrest, M. M. and Maksimov, M. S., *Theory of Incomplete Cylindrical Functions and Their Applications*, Springer, New York/Berlin, 1971.

Emittance of Semi-Infinite Scattering Medium with Refractive Index Greater than Unity

A.L. Crosbie*
University of Missouri-Rolla, Rolla, Mo.

Introduction

RECENTLY, radiant transport in liquids and solids[1] has been a problem of great interest. Several investigators[2-5] have considered the influence of the refractive index on the emission characteristics of a scattering medium. Turner and Love used the time-consuming Monte Carlo technique to study a one-dimensional planar layer[2] and a two-dimensional semi-infinite planar slab.[3] The exponential kernel approximation was used to analyze a semi-infinite[4] and a finite[5] medium. All of these studies assume isotropic scattering and an isothermal medium. The objective of the present investigation is to formulate the directional emittance of a semi-infinite medium in terms of Chandrasekhar's H-function and to obtain exact numerical results for a wide range of albedos and refractive indexes.

Formulation

The system chosen for this study is a semi-infinite planar medium at a uniform temperature which scatters isotropically and is characterized by a single scattering albedo ω_ν (ratio of scatter σ_ν to extinction β_ν coefficient) and a refractive index n_ν. The subscript ν refers to the frequency under consideration. For a semi-infinite medium with incident intensity, $I_\nu^+(0,\mu)$, the source function S_ν is given by

$$S(\tau_\nu) = (1-\omega_\nu)n_\nu^2 I_{b\nu}(T) + \frac{\omega_\nu}{2}\int_0^1 I_\nu^+(0,\mu)\exp(-\tau_\nu/\mu)\,d\mu + \frac{\omega_\nu}{2}\int_0^\infty S_\nu(t)E_1(|\tau_\nu - t|)\,dt \tag{1}$$

where $I_{b\nu}$ is the Planck blackbody function corresponding to the temperature of the medium (T), $\tau_\nu = \int_0^x \beta_\nu dx$ is optical depth into the medium, $\mu = \cos\theta$ is cosine of the polar angle, and $E_1(t) = \int_0^1 \exp(-t/\mu)(d\mu/\mu)$. Since integral Eq. (1) is linear, superposition can be applied and the source function expressed in terms of two universal functions, i.e.,

$$S_\nu(\tau_\nu) = (1-\omega_\nu)n_\nu^2 I_{b\nu}(T)B_s(\tau_\nu) + \frac{\omega_\nu}{2}\int_0^1 I_\nu^+(0,\mu)B(\tau_\nu,\mu)\,d\mu \tag{2}$$

where

$$B_s(\tau) = 1 + \frac{\omega}{2}\int_0^\infty B_s(t)E_1(|\tau - t|)\,dt \tag{3}$$

and

$$B(\tau,\mu) = \exp(-\tau/\mu) + \frac{\omega}{2}\int_0^\infty B(t,\mu)E_1(|\tau - t|)\,dt \tag{4}$$

Received Feb. 24, 1978; revision received Aug. 1, 1978.

Index categories: Radiation and Radiative Heat Transfer; Thermal Surface Properties.

*Professor, Thermal Radiative Transfer Group, Department of Mechanical and Aerospace Engineering. Member AIAA.